Review Article

Bioelectrical Impedance Devices in Clinical and Oncological Nutrition: Types, Physical Principles, and Integration with Biochemical and Pathological Biomarkers

Nooshin Abbasi[1], Marco Fiaschi[2]

1. Independent researcher; 2. MFC Elettronica, Padua, Italy

Background: Bioelectrical impedance analysis and bioelectrical impedance vector analysis (BIVA) have evolved from simple bedside estimates of body composition into sophisticated biophysical modalities capable of reflecting cellular membrane integrity, fluid distribution, and systemic vitality. In clinical and oncological nutrition, raw electrical parameters—primarily resistance (R), reactance (X_c), impedance (Z), and phase angle—exhibit direct associations with systemic inflammation, oxidative stress, and disease-related malnutrition. However, the translational utility of these parameters depends heavily on device hardware architectures, applied alternating current frequencies, measurement standardization, and their systematic integration with circulating biochemical and pathological biomarkers.

Objective: This narrative review synthesizes the biophysical principles, electronic specifications, and measurement typologies of medical-grade BIA devices, establishing an integrative framework that couples bioelectrical metrics with humoral biomarkers to improve nutritional stratification and prognostic modeling in oncology and clinical practice.

Evidence Synthesis: At low alternating current frequencies (1 to 5 kHz), the capacitive barrier of cell membranes restricts current propagation to extracellular water (ECW), whereas intermediate frequencies (50 kHz) maximize capacitive reactance, making 50 kHz the reference standard for deriving phase angle. High frequencies (100 to 1000 kHz) overcome membrane capacitance to traverse intracellular water (ICW) and total body water (TBW). Single-frequency (SF-BIA), multifrequency (MF-BIA), and bioimpedance spectroscopy devices present distinct clinical indications, with BIS and MF-BIA offering superior discrimination between true tissue depletion and fluid overload. Vectorial modeling via BIVA circumvents the confounding errors of regression equations in edematous or cachectic cancer cohorts. Across clinical populations, reduced PhA and lateral or downward BIVA vector shifts correlate strongly with elevated pro-inflammatory cytokines (interleukin-6 (IL-6), tumor necrosis factor-alpha (TNF-α)), C-reactive protein (CRP), and malondialdehyde (MDA), alongside concurrent declines in serum albumin and the Prognostic Nutritional Index (PNI).

Conclusions and Translational Value: Coupling raw bioelectrical properties (PhA, ECW/TBW, and BIVA vector quadrants) with acute-phase reactants and protein reserves enables granular identification of cachexia, sarcopenic obesity, and subclinical expansion of the extracellular compartment. Incorporating standardized PhA and vector trajectory monitoring into clinical pathways refines the Global Leadership Initiative on Malnutrition (GLIM) framework, facilitating personalized nutritional therapy and survival prediction across oncological care trajectories.

Correspondence: papers@team.qeios.com — Qeios will forward to the authors

1. Introduction and Clinical Problem Statement

Malnutrition and metabolic derangements are highly prevalent among hospitalized patients and individuals with advanced neoplastic diseases, in whom progressive weight loss, muscle wasting, and systemic inflammation combine to form the clinical picture of cancer cachexia. Accurate evaluation of body composition is essential for identifying nutritional risk, establishing metabolic phenotypes, tailoring nutritional therapy, and predicting clinical tolerance to antineoplastic regimens [1][2].

Traditional bedside anthropometric measurements, such as body weight and body mass index (BMI), are notoriously unreliable in oncology and critical illness because they cannot differentiate between skeletal muscle mass, adipose tissue, and pathologic expansions of extracellular fluid. While cross-sectional imaging modalities, including computed tomography (CT) and magnetic resonance imaging (MRI), represent reference methods for quantifying skeletal muscle mass, their high cost, radiation burden, and retrospective availability limit their routine use for serial bedside nutritional monitoring [3][4][5][6].

Bioelectrical impedance analysis [7] and bioelectrical impedance vector analysis (BIVA) have emerged as widely used, non-invasive, cost-effective, and safe bedside modalities for assessing body composition, hydration status, and cellular membrane vitality. Historically, BIA in clinical practice has relied heavily

 doi.org/10.32388/ON9IUN

on empirical regression equations designed to predict fat-free mass [8], total body water (TBW), and skeletal muscle mass [3][9].

However, these mathematical algorithms are fundamentally based on assumptions of constant tissue hydration (typically 73.2% in fat-free tissue) and stable cylindrical geometric proportions. In patients with cancer, sepsis, systemic inflammation, or organ failure, these assumptions are systematically violated due to capillary leakage, expansion of extracellular water (ECW), and cellular membrane disruption, leading to substantial prediction errors [3][4][9].

To address these limitations, clinical nutrition has shifted toward interpreting raw electrical parameters: resistance (R), reactance (X_c), total impedance (Z), and phase angle [10]. Concurrently, BIVA evaluates raw electrical properties plotted directly on a bivariate graph, providing an objective evaluation of hydration and cell mass independent of regression formulas [3][4][11].

Importantly, accumulating clinical evidence demonstrates that alterations in raw bioelectrical variables parallel humoral, inflammatory, and metabolic abnormalities. This narrative review provides a comprehensive synthesis of the biophysical and electronic principles of medical-grade BIA devices, evaluates the influence of hardware architectures and alternating current frequencies, and examines the clinical integration of raw bioelectrical metrics with circulating biomarkers of inflammation, oxidative damage, and visceral protein reserves in clinical and oncological nutrition [3][9][11][12][13][14][15].

2. Methods

2.1. Database Retrieval Framework

To ensure methodological rigor compliant with the Scale for the Assessment of Narrative Review Articles (SANRA) guidelines, a structured literature search was conducted across electronic bibliographic databases—including PubMed/MEDLINE, Scopus, Web of Science, and Cochrane CENTRAL—covering articles published up to September 2026. The search architecture combined Medical Subject Headings (MeSH) and free-text keywords covering bioelectrical impedance modalities (BIA, BIVA, BIS, phase angle, resistance, reactance), device metrology and alternating current frequencies, circulating biomarkers (C-reactive protein (CRP), interleukin-6 (IL-6), tumor necrosis factor-alpha (TNF-α), malondialdehyde (MDA), albumin, Prognostic Nutritional Index (PNI)), and clinical oncology, cachexia, or malnutrition [3][16][17].

Inclusion criteria prioritized peer-reviewed, highly cited, and methodologically sound prospective cohorts, randomized trials, international clinical consensus guidelines, and systematic reviews published in prestigious biomedical journals. Eligible studies evaluated medical-grade instrumentation reporting raw bioelectrical parameters or vector distributions alongside objective biochemical, inflammatory, or clinical endpoints in adult oncology, critical illness, or malnutrition cohorts. Non-peer-reviewed commentaries, studies relying exclusively on proprietary regression equations without reporting raw electrical metrics, uncalibrated consumer fitness devices, animal models, and investigations lacking concurrent biochemical or pathological biomarker verification were excluded [2][11].

3. Biophysical Fundamentals of Bioelectrical Tissue Conduction

3.1. Tissue Conductivity and Equivalent Circuit Modeling

Bioelectrical impedance analysis is based on the application of a weak, imperceptible alternating electrical current (typically 200 to 800 µA) to biological tissues, accompanied by the precise measurement of the resulting voltage drop to determine electrical impedance. The human body represents a complex, heterogeneous volume conductor composed of biological compartments with markedly divergent conducting properties [3][9][11].

Hydrated tissues rich in water and dissolved electrolytes—such as skeletal muscle, vascular blood volume, and parenchymal viscera—act as highly effective conductors that offer low resistance to alternating electrical current. Conversely, anhydrous tissues, including adipose tissue, dense cortical bone, and calcified structures, contain minimal freely mobile ions and exhibit high electrical resistance [9][11].

Intracellular water (ICW) also acts as an ionic resistor (R_i), but current entering this compartment must cross the surrounding cell membrane. The cellular membrane consists of a hydrophobic lipid bilayer (approximately 7 to 10 nm thick) bordered by hydrophilic protein-rich polar head groups, functioning physically as a biological dielectric capacitor (C_m) [3][9][11].

Consequently, biological tissue is electrically modeled as an extracellular resistance (R_e) in parallel with an intracellular branch containing intracellular resistance (R_i) connected in series with cell membrane capacitance (C_m) [3][9][11].

Total complex electrical impedance (Z) represents the vector sum of two orthogonal electrical components[9][11]:

doi.org/10.32388/ON9IUN

$$Z = R + jX_c$$

Where $j = \sqrt{-1}$, R is resistance, representing the pure opposition of intra- and extracellular electrolytes to current flow, and X_c is capacitive reactance, representing the opposition to current flow produced by the capacitive properties of intact cell membranes. The phase angle [10] quantifies the angular phase shift by which alternating voltage lags current due to membrane capacitance, expressed mathematically as [3][9][11]:

$$PhA = \arctan\left(\frac{x_c}{R}\right) \times \left(\frac{180^0}{\pi}\right)$$

Physiologically, PhA serves as a biophysical index of cell membrane integrity, active body cell mass (BCM), and the distribution of body fluids between intra- and extracellular spaces. High PhA values reflect large quantities of intact, polarized cellular membranes and dense body cell mass [3][11].

In contrast, low PhA values indicate structural membrane breakdown, loss of selective permeability, intracellular fluid depletion, or expanded extracellular water volumes, characteristics typical of systemic inflammation, malnutrition, and cachexia [3][9][11][18][19].

3.2. Frequency-Dependent Dispersion and Fluid Compartments

The electrical conduction pathway through biological tissue depends directly on the frequency of the applied alternating current, a phenomenon described as electrical dispersion. Across radiofrequency spectra, biological tissues exhibit distinct dispersion zones: α-dispersion occurs at low frequencies (< 1 kHz) due to ionic diffusion and counter-ion polarization around cell surfaces; β-dispersion spans intermediate and radio frequencies (1 kHz to several hundred MHz) dominated by the polarization of cellular membranes and structural interfaces; and γ-dispersion emerges at gigahertz frequencies governed by water dipole relaxation [3][9][11].

In clinical bioimpedance, the working frequency spectrum operates within the β-dispersion range. At very low frequencies (1 to 5 kHz), the capacitive reactance of the lipid bilayer is high[3][11]:

$$x_c = \frac{1}{2\pi_f C_m}$$

As a result, cell membranes function as electrical insulators. The alternating current cannot penetrate the lipid bilayer and is confined entirely to extracellular fluid channels. Measurements taken at low frequencies therefore reflect the resistance and volume of extracellular water (ECW) [3][9][11].

At intermediate frequencies (approximately 50 kHz), the applied frequency closely matches the dielectric properties of human cell membranes, maximizing capacitive reactance (X_c). At 50 kHz, the current passes through both extracellular fluid and a substantial fraction of healthy cell membranes, providing an integrated assessment of total body water, cellular membrane integrity, and BCM. This biophysical property makes 50 kHz the standard reference frequency for deriving PhA in single-frequency and vector analyses [4][9][11].

At high and ultra-high frequencies (100 to 200 kHz, extending up to 1000 kHz in spectroscopy systems), the capacitive reactance of the lipid bilayer drops toward zero (X_c → 0). The alternating current easily bridges the membrane capacitor and conducts through both intracellular and extracellular fluids [3][9][11].

High-frequency resistance measurements reflect total body water (TBW). By mathematically resolving low-frequency resistance ($R_0 \approx R_e$) and high-frequency resistance ($R_\infty \approx (R_e \times R_i) / (R_e + R_i)$), multifrequency systems calculate intracellular water as [4][11]:

$$ICW = TBW - ECW$$

This enables the calculation of the extracellular-to-total body water ratio (ECW/TBW), a metric for evaluating cellular hydration and fluid redistribution [4][11][20].

Mathematically, tissue impedance across continuous frequencies is characterized by the semi-empirical Cole-Cole model [9][11][20]:

$$z(\omega) = R_\infty + \frac{R_0 - R_\infty}{1 + (j\omega\tau)^\alpha}$$

Where $\omega = 2\pi f$ is angular frequency, τ is the characteristic relaxation time constant of the cellular system, R_0 is theoretical resistance at zero frequency, R_∞ is resistance at infinite frequency, and α ($0 < \alpha \leq 1$) describes the distribution of relaxation times and non-ideal capacitive properties across heterogeneous cell populations [3][9].

In disease states, systemic inflammation, oxidative stress, and structural tissue catabolism alter these Cole-Cole parameters. This leads to a flattened impedance locus, lowered characteristic frequency (f_c), and a depression of the Cole arc, reflecting cellular degradation and extracellular fluid expansion [3]

 doi.org/10.32388/ON9IUN

[9][11].

4. Hardware Typology, Frequency Spectra, and Metrological Standardization: Single-frequency versus multifrequency and spectroscopy devices

4.1. Single-Frequency, Multi-Frequency, and Spectroscopy Modalities

Medical-grade bioelectrical impedance instruments are classified into three primary categories based on frequency generation, signal acquisition, and analytical processing [3][4][11]:

1. Single-Frequency BIA (SF-BIA) devices operate at a fixed alternating current frequency, universally standardized at 50 kHz. SF-BIA instruments directly measure resistance (R), capacitive reactance (X_c), impedance (Z), and phase angle [10]. Because 50 kHz maximizes capacitive reactance while maintaining high signal stability, SF-BIA represents the historical and validated standard for classical bioelectrical impedance vector analysis (BIVA) [1][3][4][9][11].

   In clinically stable patients, SF-BIA provides reliable estimates of fat-free mass and body cell mass. However, because it operates at a single frequency, it cannot directly measure fluid distribution between intracellular and extracellular compartments during acute hydration shifts [3][4][9][11].
2. Multi-Frequency BIA (MF-BIA) devices apply several discrete alternating current frequencies, typically including 5 kHz, 50 kHz, 100 kHz, 200 kHz, and 500 kHz. By measuring tissue resistance across this spectrum, MF-BIA models low-frequency extracellular conduction alongside high-frequency total body conduction [3][4][11].

   This enables direct calculation of ECW, ICW, TBW, and the ECW/TBW ratio, making MF-BIA valuable for identifying fluid retention, overhydration, and sarcopenic fluid accumulation in surgical, oncological, and critically ill cohorts [2][3][4].
3. Bioimpedance Spectroscopy [10] devices scan a continuous spectrum of alternating frequencies, typically between 1 kHz and 1000 kHz, acquiring dozens to hundreds of discrete impedance data points. Using nonlinear complex curve fitting, BIS plots the data on the Cole-Cole plane to calculate theoretical resistances at zero frequency (R_0) and infinite frequency (R_∞) alongside the characteristic membrane frequency (f_c) [3][9][11][20].

BIS provides the most accurate biophysical separation of intracellular and extracellular fluid volumes without relying on population-based empirical regression equations. It is the reference method for diagnosing lymphedema, monitoring dialysis ultrafiltration, and evaluating advanced cachexia accompanied by severe fluid third-spacing [1][3][11].

4.2. Electrode Geometry, Positioning, and Patient Postural Dynamics

The physical interface between the device and biological tissue strongly influences measurement precision and clinical reproducibility. Most medical-grade devices employ a tetrapolar electrode montage [3][4][9][20].

In this configuration, two outer drive electrodes inject a constant alternating current into the body, while two inner sense electrodes measure the resulting voltage drop. This tetrapolar arrangement eliminates the influence of electrode contact impedance and skin-electrode polarization resistance from the voltage measurement circuit, which would otherwise introduce major artifacts into measured resistance and reactance [3][9][11].

Tetrapolar configurations place adhesive electrodes on the dorsal surfaces of the wrist and ankle on the same side of the body [3][9][11]:

- The hand injector electrode is positioned over the third metacarpophalangeal joint, while the sensing electrode is placed across the dorsal wrist crease between the styloid processes of the radius and ulna [3][9][11].
- The foot injector electrode is positioned over the third metatarsophalangeal joint, with the sensing electrode placed across the anterior surface of the ankle between the medial and lateral malleoli [3][9][11].
- A minimum inter-electrode distance of 5 cm between injecting and sensing terminals is required to avoid current density distribution artifacts [3][9][11].

Octopolar or segmental devices employ eight contact points (four on the hands, four on the feet), incorporating both palm grips and footplates. This configuration switches current injection and sensing pathways across different anatomical pairs, enabling isolated impedance measurements of the right arm, left arm, trunk, right leg, and left leg [3][11].

 doi.org/10.32388/ON9IUN

Segmental analysis is helpful for identifying localized muscle atrophy or asymmetric edema. However, because the trunk contributes only 10% to 15% of whole-body resistance despite accounting for roughly 50% of total body mass, segmental trunk impedance measurements have a lower signal-to-noise ratio than whole-body limb-to-limb configurations [3][11].

Patient posture during measurement introduces significant physiological variability. Supine (clinostatic) measurements, conducted after 5 to 10 minutes of horizontal rest, allow gravity-dependent fluid shifts to equilibrate between interstitial and intravascular spaces, while relaxing postural muscles. This makes supine positioning the standard for hospitalized, frail, or bedridden oncological patients [2][3][9].

Standing platforms are common in outpatient nutrition clinics and fitness centers due to operational convenience. However, standing upright induces rapid downward fluid redistribution into the lower extremities, increases hydrostatic microvascular filtration, and elevates postural muscle tone in the lower limbs and trunk. These changes can alter lower-limb resistance and reactance by 5% to 8% within minutes, requiring strict operational standardization when monitoring patients over time [3][11][20].

4.3. Electronic Shielding, Power Isolation, and Signal Metrology

From an electronic engineering perspective, the stability and fidelity of the measured impedance signal depend directly on device power isolation, circuit design, and electrode interface stability [3][11][21]:

Power line interference presents a major challenge in clinical settings. Instruments powered directly from alternating current mains lines (110-230 V at 50/60 Hz) can pick up common-mode line noise that distorts micro-ampere bioimpedance signals. This interference disproportionately affects low-frequency measurements and capacitive reactance (X_c), introducing significant errors into derived phase angles [3][11][20].

Medical-grade systems resolve this using high-isolation internal power supplies, battery-powered architectures, and optical isolation barriers that separate patient-facing analog measurement circuitry from digital processing units [3].

Electrical safety compliance requires adherence to the IEC 60601-1 standard for medical electrical equipment. BIA devices are classified as Type BF or Type CF applied parts, with strict limits on patient leakage currents (under normal conditions <100 µA, and under single-fault conditions <500 µA). These safety features prevent microshock hazards, enabling safe monitoring in high-risk patients, including those with indwelling vascular catheters [3][11][16][21].

However, external electrical fields and high-frequency surgical units can disrupt impedance circuitry, and the safe use of BIA in patients with cardiac pacemakers or implantable cardioverter-defibrillators (ICDs) requires prior clinical clearance, as high-frequency alternating test currents could theoretically interfere with cardiac sensing algorithms [3][6][22].

Electrode interface quality also plays an important role in measurement accuracy. Low-grade or dried adhesive electrodes increase contact impedance, while polarization at the metal-electrolyte interface causes phase shifts and artificially inflates measured resistance. Medical protocols require high-conductivity Ag/AgCl adhesive electrodes containing conductive hydrogel, paired with standard skin preparation (cleansing with 70% isopropyl alcohol to remove surface sebum and dead epidermal layers) [3][11].

Hardware calibration must be verified daily using precision resistor-capacitor (RC) calibration test circuits with known electrical values (such as R = 380 Ω and X_c = 45 Ω) to confirm circuit linearity and measurement precision across working frequency bands [3][23].

4.4. Low-Frequency Limitations and High-Frequency Advantages

Selecting the appropriate alternating current frequency requires balancing metrological signal quality with biological compartment sensitivity. Very low frequencies (around 1 kHz) are theoretically ideal for isolating extracellular water (ECW) because cell membranes prevent intracellular current penetration [3][9][11].

However, below 2 to 3 kHz, skin-electrode interface impedance and polarization effects increase exponentially, which introduces noise and lowers measurement reproducibility. To avoid these polarization artifacts while maintaining sensitivity to extracellular fluid, modern clinical devices typically operate their lowest discrete frequency at 5 kHz [1][3][9][14][20][21][24][25].

Conversely, intermediate and high frequencies (50 kHz to 500 kHz) overcome skin-contact impedance, providing high signal-to-noise ratios and consistent biological measurements. Because 50 kHz coincides with the peak of capacitive reactance (X_c) in healthy skeletal muscle, it produces clear phase-shift signals that correlate strongly with cell membrane mass and integrity [3][9][11].

doi.org/10.32388/ON9IUN

Frequencies above 100 kHz bridge the cell membrane capacitor, allowing the current to pass freely through intracellular fluid and providing accurate measurements of total body water (TBW) [1][3][9][13][19][20][25][26].

5. Vectorial Bioimpedance: The R-X_c Graph and Hydration Independence

Bioelectrical impedance vector analysis (BIVA), introduced by Piccoli and colleagues, is a reference-free methodology that avoids the assumptions of conventional regression equations. BIVA plots raw resistance and reactance, normalized to patient height (R/H and X_c/H, in Ω/m), as a planar vector on an R-X_c Cartesian coordinate system [1][11][16][19][27][28].

Individual vectors are evaluated against population-specific bivariate reference tolerance ellipses (50%, 75%, and 95% confidence intervals) derived from healthy reference cohorts matched for sex, age, and race [1][11][29][30].

The position of an individual impedance vector on the R-X_c Cartesian plane provides an objective, two-dimensional assessment of tissue hydration and cellular mass independent of empirical prediction equations (Figure 1) [1][11][31]:

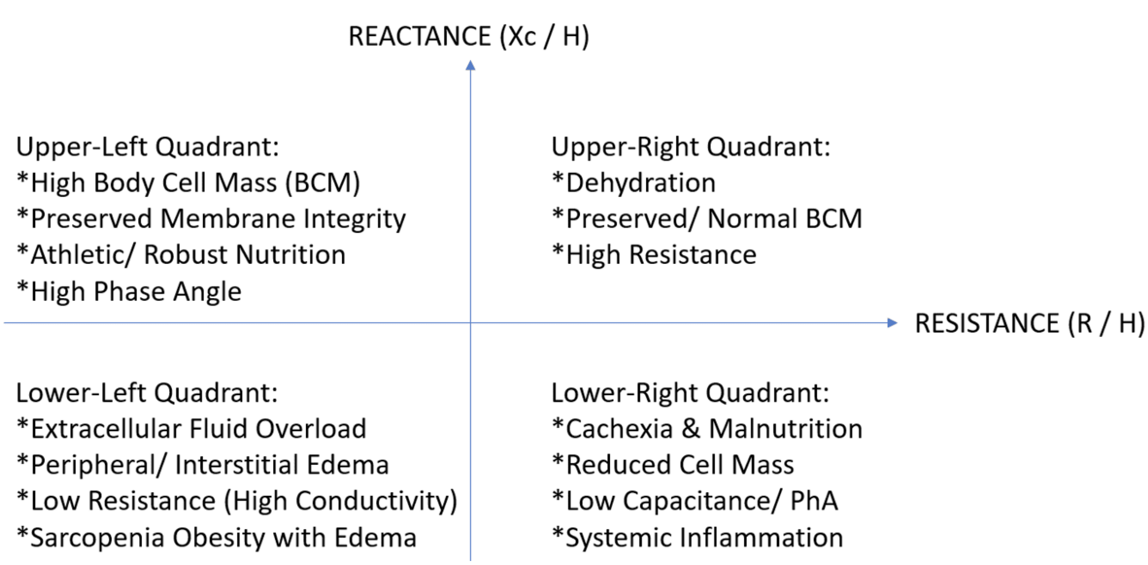

Figure 1. The Bioelectrical Impedance Vector Analysis (R-X_c) Nomogram: Reference Tolerance Ellipses and Clinical Quadrant Phenotypes

Vector displacement along the minor axis reflects differences in cellular mass, membrane integrity, and soft-tissue structure. Lateral and downward displacement toward the right indicates reduced capacitive reactance and low phase angle, reflecting loss of body cell mass, structural membrane degradation, and expansion of extracellular water relative to intracellular volume [1][11].

Displacement toward the left reflects preserved or increased cell mass with high membrane capacitance, typical of muscular, well-nourished individuals [1][11].

The four quadrants of the BIVA Cartesian plane correspond to distinct clinical phenotypes [1][11]:

- Upper-Left Quadrant (Low R/H, High X_c/H): Athletic, well-nourished individuals characterized by high body cell mass, intact cellular membranes, and normal or slightly elevated total body water.
- Upper-Right Quadrant (High R/H, High X_c/H): True tissue dehydration, characterized by reduced fluid volume alongside preserved cell mass and intact membranes.
- Lower-Left Quadrant (Low R/H, Low X_c/H): Fluid overload and edema, characterized by expanded extracellular fluid, low systemic resistance, and preserved or mildly diminished cell mass.
- Lower-Right Quadrant (High R/H or Intermediate R/H, Low X_c/H): Disease-associated cachexia, advanced malnutrition, and systemic inflammation. These vectors fall outside the 75% or 95% tolerance ellipses, reflecting severe depletion of metabolically active cell mass, membrane breakdown, and an elevated ECW/ICW ratio.

 doi.org/10.32388/ON9IUN

In cancer care, intensive care, and nephrology, BIVA provides a practical alternative to regression equations, which tend to overestimate muscle mass in the presence of subclinical edema. Plotting sequential measurements on the BIVA plane allows clinicians to track dynamic trajectory vectors over time, helping distinguish true anabolic tissue recovery from fluid accumulation during nutritional therapy [1][4][11][19][27].

6. Convergence of Bioelectrical Properties with Pathological Biomarkers

The biological continuum connecting circulating pro-inflammatory mediators, free-radical membrane injury, and visceral protein wasting to quantifiable biophysical impedance alterations is outlined in Table 1 [1][4][11].

PATHOPHYSIOLOGICAL AXIS: MOLECULAR TO ELECTRICAL		
Humoral & Inflammatory State	**Cellular & Membrane Impact**	**Bioelectrical Signature**
• High IL-6, TNF-α, CRP • High Malondialdehyde (MDA) • Low Albumin & PNI • Depleted Visceral Proteins	• Capillary hyperpermeability • Lipid peroxidation of bilayer • Loss of selective permeability • Intracellular fluid leakage	• Decreased Reactance (X_c) • Depressed Phase Angle • Elevated ECW/TBW ratio • BIVA vector down-right

Table 1. Pathophysiological Axis Linking Humoral Inflammatory Cascades and Oxidative Stress to Cellular Membrane Breakdown and Bioelectrical Impedance Signatures

6.1. Phase Angle and Systemic Meta-Inflammation

Systemic inflammation is a primary driver of cancer cachexia, muscle wasting, and disease-related malnutrition. Pro-inflammatory cytokines, including interleukin-6 (IL-6), tumor necrosis factor-alpha (TNF-α), and interleukin-1beta (IL-1β), stimulate hepatic synthesis of positive acute-phase reactants—most notably C-reactive protein (CRP)—while downregulating the synthesis of constitutive hepatic proteins such as albumin and transferrin [2][9][11][23][32].

At the cellular level, these cytokines alter vascular endothelium and cell membrane properties. They increase endothelial and cellular membrane permeability, cause intracellular potassium leakage, disrupt active sodium-potassium adenosine triphosphatase (Na^+/K^+-ATPase) ion pumps, and diminish resting transmembrane electrical potential [2][3][11].

This loss of membrane polarization decreases the capacitance of the lipid bilayer, reducing capacitive reactance (X_c). At the same time, increased microvascular permeability promotes the shift of albumin and plasma water into the interstitial space, expanding extracellular water (ECW) and lowering low-frequency electrical resistance (R)[4][9][11].

Because phase angle is derived from the arctangent ratio of reactance to resistance (PhA = $\arctan(\frac{X_c}{R}) \times (\frac{180^\circ}{\pi})$), this combined drop in reactance and shift in fluid balance significantly lowers the measured phase angle [3][11].

Clinical studies across diverse patient populations consistently demonstrate an inverse relationship between PhA and inflammatory biomarkers [2][4][11]:

- Barrea and colleagues demonstrated in cohorts with obesity and meta-inflammation that reduced PhA correlates strongly with elevated high-sensitivity CRP (hs-CRP), TNF-α, and IL-6. Receiver operating characteristic curves identified sex-specific PhA cut-offs ($\leq 5.5°$ for men and $\leq 5.4°$ for women) that independently predicted elevated hs-CRP, even after adjusting for age, waist circumference, and dietary patterns [4].
- Stobäus and colleagues analyzed 777 hospitalized patients and found that serum CRP and nutritional risk were the strongest independent determinants of both raw PhA and standardized phase angle (SPhA), accounting for more variance than the primary disease diagnosis [3].
- In gastrointestinal oncological surgery and critical illness, Lee and Kim reported that PhA measured on postoperative day 1 was inversely correlated with serum CRP, procalcitonin, and presepsin. Patients with low PhA experienced significantly higher rates of postoperative surgical site infections, sepsis, and delayed recovery [12].
- In systemic inflammatory response syndrome (SIRS) and septic shock, Swaraj and colleagues observed that a PhA < 4.0° strongly predicted 28-day mortality, reflecting the combined impact of systemic inflammation, loss of membrane potential, and diffuse capillary leakage [33].

doi.org/10.32388/ON9IUN

- A systematic review in cardiovascular diseases found that PhA was inversely associated with CRP and TNF-α in most included studies, supporting its potential use as an indirect marker of inflammation and a tool for therapeutic planning. In gastrointestinal surgery, PhA measured on postoperative day 1 was strongly negatively correlated with CRP, procalcitonin, and presepsin, and lower PhA predicted postoperative infections, emphasizing the role of PhA as a biomarker of inflammatory complications [12][32].

6.2. Phase Angle, Lipid Peroxidation, and Oxidative Stress

Oxidative stress, characterized by an imbalance between the production of reactive oxygen and nitrogen species (RONS) and endogenous antioxidant defenses, plays a key role in membrane degradation and muscle wasting. Biological cell membranes are particularly susceptible to free radical damage because their phospholipid bilayers are rich in polyunsaturated fatty acids (PUFAs)[11][15].

When exposed to excessive superoxide radicals, hydrogen peroxide, and hydroxyl ions, PUFAs undergo lipid peroxidation, producing toxic breakdown products such as malondialdehyde (MDA) and 4-hydroxynonenal (4-HNE)[9][34].

Lipid peroxidation degrades the hydrophobic membrane core, forms cross-linked protein adducts, reduces membrane fluidity, and creates hydrophilic pores that collapse the transmembrane potential. This structural degradation reduces the electrical capacitance (C_m) of the membrane, leading to a decline in bioelectrical reactance (X_c) and a corresponding decrease in PhA [9][34].

In a prospective study of breast cancer patients undergoing anthracycline- and taxane-based chemotherapy, da Silva and colleagues directly linked bioelectrical variables with oxidative stress and antioxidant biomarkers. Phase angle correlated positively with total antioxidant capacity (assayed by 2,2-diphenyl-1-picrylhydrazyl, DPPH) and serum albumin, while correlating inversely with serum MDA levels and CRP [1][9][11].

Multivariate regression analysis revealed that circulating MDA, DPPH, CRP, fat mass, and the TBW/ECW ratio together accounted for over 50% of the variance in PhA during chemotherapy. Because chemotherapy regimens generate significant oxidative damage, these findings indicate that serial PhA measurements can serve as a non-invasive bedside tool to identify oxidative and inflammatory membrane injury [1][9][15].

6.3. Visceral Protein Depletion, Hypoalbuminemia, and Composite Indices

Serum albumin has traditionally served as a biochemical marker of nutritional status, but in clinical illness, circulating concentrations are predominantly governed by systemic inflammation, hepatic reprioritization, and transcapillary escape. Pro-inflammatory states accelerate the transcapillary escape rate of albumin into the interstitial space, expanding extracellular water while depressing circulating albumin levels [2][15][27][35].

Consequently, hypoalbuminemia is frequently accompanied by lower tissue resistance (R) and decreased reactance (X_c), leading to a downward and rightward vector shift on the BIVA graph and a marked drop in PhA [4][16][19][36].

Across solid tumors—including lung, gastrointestinal, pancreatic, and colorectal cancers—studies demonstrate consistent positive correlations between PhA and serum albumin, prealbumin, transferrin, total cholesterol, and absolute lymphocyte counts. In non-small cell lung cancer, Prete and colleagues showed that lower PhA was associated with poor functional status, rapid weight loss, and hypoalbuminemia, serving as an independent predictor of shorter progression-free and overall survival [3][5][8][16][22][37].

These relationships extend to validated composite prognostic scores, such as the Prognostic Nutritional Index (PNI)[38]:

PNI = 10 × Albumin (g/dL) + 0.005 × Total Lymphocyte Count (/μL)

PNI integrates hepatic protein reserve with host immunologic competence. When evaluated alongside BIA, PhA and PNI show strong positive correlations [1].

Combining both modalities provides complementary prognostic insight: while PNI captures circulating protein reserves and immunological status, PhA and BIVA reflect peripheral cellular architecture, membrane integrity, and tissue fluid distribution. Patients presenting with both low PNI and depressed PhA experience the highest rates of chemotherapy toxicity, hospital readmissions, and early mortality [4][16][22][23][39].

7. Integrated Multi-Marker Matrix

The following matrix shown in Table 2 integrates raw bioelectrical properties, physical mechanisms, associated humoral biomarkers, and clinical interpretations across oncological and critical care settings [3][5][9][13][38].

doi.org/10.32388/ON9IUN

Bioelectrical Parameter	Biophysical and Physiological Mechanism	Associated Circulating Biomarkers	Clinical and Oncological Interpretation
PhA = arctan($\frac{X_c}{R}$)×($\frac{180^\circ}{\pi}$),	Reflects the capacitive charge storage of cell membranes and the proportion of metabolically active body cell mass relative to total fluid volume.	Inversely correlated: hs-CRP, IL-6, TNF- α, MDA, Procalcitonin. Positively correlated: Serum Albumin, Prealbumin, Transferrin, Total Lymphocyte Count.	Low PhA (<4.5 to 5.0 degrees) or SPhA < -1.65 reflects membrane degradation, systemic catabolism, persistent inflammation, and elevated mortality across advanced neoplasms.
Extracellular-to-Total Body Water Ratio (ECW/TBW)	Low-frequency resistance (Re) reflects interstitial and intravascular fluid expansion relative to high-frequency whole-body conduction.	Positively correlated: CRP, Interleukin-1β, Cortisol, Natriuretic Peptides (BNP/NT-proBNP). Inversely correlated: Serum Albumin, Hemoglobin.	Elevated ECW/TBW (>0.390 to 0.400) indicates subclinical extracellular fluid expansion, increased capillary permeability, third-spacing, and systemic inflammation in cachectic patients.
Capacitive Reactance (Xc) Normalized to Height (Xc/H)	Directly measures the total electrical capacitance and structural integrity of cellular membranes across skeletal muscle and visceral organs.	Positively correlated: Insulin-like Growth Factor 1 (IGF-1), Skeletal Troponin, Serum Creatinine. Inversely correlated: Malondialdehyde (MDA), Protein Carbonyls.	Depressed Xc/H indicates marked depletion of active body cell mass, extensive myocyte membrane degradation, and severe muscle wasting (sarcopenia and cachexia).
BIVA Vector Trajectory (R/H vs. Xc/H bivariate plane)	Simultaneously tracks shifts in tissue hydration (displacement along the major axis) and cellular mass/membrane integrity (displacement along the minor axis).	Downward/Right Shift: Correlates with elevated CRP, high systemic immune-inflammation index (SII), hypoalbuminemia. Upward/Left Shift: Correlates with preserved visceral protein synthesis and normal inflammatory markers.	Characterizes four distinct clinical hydration-nutrition phenotypes: athletic/eutrophic (upper-left), dehydration (upper-right), fluid overload/edema (lower-left), and edematous cachexia with severe systemic inflammation (lower-right).
Prognostic Nutritional Index Integration (PhA + PNI Coupling)	Integrates biophysical cellular health [2] with systemic immune competence and hepatic visceral protein synthetic capacity.	Direct Components: Serum Albumin (g/L) and Total Lymphocyte Count (x 10^9/L): PNI = 10 × Albumin + 0.005 × Lymphocytes.	Identifies discordant clinical profiles (e.g., preserved albumin alongside depressed PhA due to acute inflammatory fluid shifts); dual impairment identifies patients at high risk for dose-limiting toxicities and poor survival.

Table 2. Integrated Multi-Marker Matrix: Biophysical Conduction Mechanisms, Circulating Biomarker Correlates, and Oncological Clinical Interpretations of Bioelectrical Parameters

8. Translational Clinical Applications in Oncology and Critical Illness

8.1. Phenotyping Cancer Cachexia, Sarcopenic Obesity, and Fluid Overload

The clinical phenotype of the oncological patient is rarely static; metabolic derangements can cause rapid shifts between tissue wasting, fluid overload, and altered fat distribution. Standard anthropometric parameters regularly miss these transitions [4][11][20].

For example, in sarcopenic obesity, patients retain large quantities of adipose tissue while experiencing progressive skeletal muscle atrophy. Similarly, patients receiving intravenous fluids, corticosteroids, or platinum-based chemotherapy may maintain stable body weight while secretly accumulating several liters of extracellular fluid, masking skeletal muscle loss [1][4][11][22].

BIA and BIVA resolve these diagnostic challenges by separating tissue mass from fluid volume[1][11]:

- In simple dehydration, tissue resistance (R/H) increases while reactance (X_c/H) remains relatively preserved, shifting the vector upward and to the right along the major axis [1][11].
- In fluid overload and expanding edema, whole-body resistance drops, shifting the vector downward and to the left [1][11].
- In refractory cancer cachexia, the vector moves into the lower-right quadrant, reflecting depleted cell mass, membrane breakdown, and an expanded ECW/ICW ratio [1][11].

 doi.org/10.32388/ON9IUN

Identifying this lower-right vector shift alerts the clinical team that an apparent stability in body weight may actually reflect subclinical fluid retention masking progressive muscle wasting [1][11][16].

8.2. Standardized Phase Angle (SPhA) as a Prognostic Risk-Adjusted Metric

A practical challenge when applying raw PhA in clinical settings is its physiological variation with age, sex, and BMI. Biological males display higher baseline PhA values than females due to greater muscle cell mass and higher membrane capacitance, whereas advancing age leads to a natural decline in PhA from gradual myocyte loss and subclinical expansion of the extracellular compartment [3][11].

BMI also influences raw PhA: values increase from low weight up to a BMI of approximately 30 to 35 kg/m^2, after which severe obesity leads to a decline in PhA driven by chronic meta-inflammation and expanded extracellular fluid volumes [3][11].

To eliminate these physiological confounders, clinicians should standardize raw PhA against healthy, reference population databases matched for sex, age, and BMI [11][40]:

$$SPhA = \frac{PhA_{measured} - PhA_{reference}}{SD_{reference}}$$

Expressed as a standard deviation score (z-score), PhA provides a risk-adjusted metric that is comparable across diverse clinical cohorts [3][5].

Multiple clinical investigations show that an SPhA < -1.65 (falling below the 5th percentile) independently predicts impaired functional status, reduced quality of life, increased susceptibility to dose-limiting chemotherapy toxicities, and significantly shorter overall survival across varied neoplastic malignancies. Incorporating SPhA into oncological evaluation provides an objective, risk-adjusted threshold for early supportive and nutritional interventions [3][4][5][11][23].

8.3. Diagnostic Integration with the GLIM Framework and Bedside Muscle Ultrasound

To achieve diagnostic consensus across clinical settings, the Global Leadership Initiative on Malnutrition (GLIM) established a two-step framework for diagnosing malnutrition: initial screening using validated tools (such as NRS-2002 or MUST), followed by formal assessment requiring at least one phenotypic criterion (involuntary weight loss, low BMI, or reduced muscle mass) and at least one etiologic criterion (reduced food intake/assimilation or disease-related systemic inflammation) [6][23][41].

Bioelectrical impedance directly supports this diagnostic framework:

1. Phenotypic Assessment: BIA estimates fat-free mass and appendicular skeletal muscle mass, which are indexed to height squared (FFMI or ASMI) to satisfy the GLIM reduced muscle mass criterion using established diagnostic cut-offs (FFMI < 17 kg/m^2 for men and < 15 kg/m^2 for women; ASMI < 7.0 kg/m^2 for men and < 5.5 kg/m^2 for women) [6].
2. Etiologic Assessment: While acute inflammation is traditionally confirmed via laboratory CRP or cytokine assays, an abnormal bioelectrical signature —specifically a low PhA or elevated ECW/TBW ratio—serves as an objective bedside surrogate of chronic systemic inflammation, identifying cellular injury even before laboratory results are finalized [3][11][20].

The clinical utility of BIA can be further enhanced by pairing it with point-of-care nutritional ultrasound of the rectus femoris muscle. While BIA and BIVA evaluate whole-body fluid distribution and cellular membrane capacitance, bedside muscle ultrasound provides direct anatomical visualization of muscle architecture [23][40][42][43].

Using high-frequency linear probes (10 to 12 MHz), clinicians can measure the rectus femoris cross-sectional area (RF-CSA) and muscle layer thickness, while assessing muscle echogenicity. Hyperechogenicity reflects intramuscular adipose tissue infiltration and fibrous degeneration [7][23][40].

Combining bioimpedance with ultrasound creates an objective morphofunctional assessment: BIVA detects fluid retention and cellular membrane compromise, while ultrasound confirms physical myocyte wasting and structural tissue quality [5][10][23].

8.4. Four-Tiered Decision Framework for Clinical Nutrition Practice

To integrate these biophysical principles into routine clinical practice, nutritionists and oncology teams can implement a four-tiered decision model:

1. **Tier 1: Standardized Baseline Assessment.** Perform measurements using a calibrated medical-grade device with direct access to raw R, X_c, Z, and PhA. Follow standardized clinical protocols: patient in a supine position after 5 to 10 minutes of rest, clean skin interfaces, and tetrapolar Ag/AgCl

doi.org/10.32388/ON9IUN

adhesive electrodes. Obtain concurrent laboratory panels, including serum albumin, hs-CRP, and complete blood counts to calculate PNI [3][5][9][11][13][23].

2. **Tier 2: Phenotypic Classification.** Plot height-normalized vectors (R/H versus X_c/H) on reference tolerance ellipses to classify the patient into one of the four BIVA quadrants (eutrophic, dehydrated, edematous, or cachectic-inflammatory). Calculate SPhA to control for age, sex, and BMI. Integrate these metrics into the GLIM framework to verify whether phenotypic muscle loss and etiologic inflammation criteria are satisfied [1][11][19][27][40].
3. **Tier 3: Dynamic Serial Monitoring.** Track bioimpedance trajectories across cycles of chemotherapy, radiation, or nutritional therapy. An upward-left vector movement indicates cellular preservation and a positive response to nutritional support. A downward-right vector shift or an acute drop in PhA $\geq$ 0.90° signals active tissue catabolism, loss of membrane integrity, or subclinical capillary leak, alerting clinicians to impending clinical decline before overt functional impairment occurs [1][4][12][15][16].
4. **Tier 4: Targeted Risk Stratification.** Combine bioelectrical and humoral metrics to stratify patients into risk tiers. Patients presenting with both low SPhA (< -1.65) and low PNI have a significantly elevated risk of severe chemotherapy toxicity, postoperative infections, and early mortality. These high-risk individuals should be prioritized for multimodal supportive care, including targeted medical nutrition, anti-inflammatory therapies, tailored exercise protocols, and potential chemotherapy dose adaptations [1][3][4][9][11][33].

This structured use of BIA/BIVA transforms devices from simple body composition tools into integrative instruments for assessing cellular health, malnutrition, and inflammation.

9. Novelty Appraisal and Literature Benchmarking

9.1. Core Conceptual Novelty

The primary scientific merit of this review lies in establishing an integrative biophysical-biochemical framework that connects electrical circuit mechanics, hardware engineering, cellular physiology, and circulating clinical biomarkers. Existing literature in the field has largely remained divided into two isolated disciplines [3][11]:

- Biophysical and biomedical engineering publications focus heavily on Cole-Cole modeling, electrical dispersion, instrumentation circuitry, and electrode skin impedance, but typically evaluate these concepts in healthy volunteers or bench models without addressing clinical oncology or cachexia [3][9][11].
- Clinical nutrition publications frequently utilize BIA as a simple bedside tool, relying on empirical regression formulas to estimate kilograms of skeletal muscle mass while treating the instrument as a black box. In doing so, they often ignore how fluid shifts and membrane disruption in advanced disease distort these regression calculations [1][3][4][11].

This review bridges these domains by examining the biophysical mechanisms that explain why empirical regression formulas fail in unstable clinical conditions, while explaining how raw electrical properties (R, X_c, PhA) directly reflect cellular pathology [3][11].

By connecting the physics of membrane capacitance (C_m) to cytokine-mediated endothelial leakage, lipid peroxidation of phospholipid bilayers, and visceral protein synthesis, this review provides a mechanistic rationale for using raw bioimpedance metrics alongside humoral biomarkers [1][3][9].

A detailed comparison highlighting the conceptual and methodological divergence between conventional clinical BIA literature, biophysical engineering publications, and the integrative framework established in this review is detailed in Table (3) [21][26].

doi.org/10.32388/ON9IUN

CONCEPTUAL ARCHITECTURE: BRIDGING THE GAP		
Conventional BIA Literature (Clinical Nutrition)	**Biomedical Engineering (Biophysical Domain)**	**Integrative Framework (Present Review)**
*Black-box empirical equations *Predicts FFM / TBW / Muscle kg *Fails during fluid shifts *Limited consideration of underlying electronics *Often overlooks direct link to circulating biomarkers	*Cole-Cole impedance modeling *Alternating frequency circuits *Dielectric dispersion (alpha, beta, gamma) *Tested primarily in bench or healthy human cohorts *Lacks translational oncology	*Explains equation breakdown *Links raw R, Xc, and PhA directly to cell membrane integrity and fluid shifts *Integrates circuit physics with cytokines, MDA, albumin, and PNI

Table 3. Conceptual Architecture: Methodological Comparison Between Conventional Clinical BIA Literature, Biophysical Engineering Modalities, and the Integrative Framework of the Present Review

9.2. Benchmarking Against Recent High-Impact Literature (2022–2026)

A comparative evaluation against literature published between 2022 and 2026 underscores the timeliness and unique focus of this synthesis:

The foundational review by da Silva et al. (2023) detailed the physiological determinants of phase angle, emphasizing its links with systemic inflammation and oxidative stress. Concurrently, their prospective clinical trial in breast cancer patients receiving anthracycline chemotherapy demonstrated that PhA correlates with circulating MDA, total antioxidant capacity (DPPH), and albumin [1][9][11].

The present review builds upon these findings by analyzing how hardware engineering, frequency selection (low vs. intermediate vs. spectroscopy), and electrode interface polarization influence the fidelity of these biomarker correlations [3][11].

Systematic reviews by Branco et al. (2023) and Prete et al. (2024) surveyed BIA applications in oncology, documenting that lower PhA predicts poorer survival and longer hospitalizations. This review complements their clinical findings by detailing the underlying equivalent circuit physics, illustrating how inflammatory capillary leakage and lipid membrane degradation directly decrease capacitive reactance and induce vector shifts on the BIVA plane [1][4][9][16][25].

Large-scale clinical evaluations, including the multicenter analysis by Diniz et al. (2025) involving over 19,000 cancer patients, as well as recent methodological papers by Dupertuis et al. (2025) and Dal Bello et al. (2025), have highlighted significant measurement discrepancies across commercial BIA instruments, advocating for reference-free vector analysis [4][11][16][26][27].

The present review synthesizes these modern developments into an actionable, four-tiered clinical roadmap that aligns raw bioimpedance parameters with the GLIM diagnostic framework and bedside muscle ultrasound [5][23].

10. Conclusions and Translational Research Horizons

Medical-grade bioelectrical impedance analysis and bioelectrical impedance vector analysis provide an objective, non-invasive methodology for evaluating body composition, fluid distribution, and cellular vitality in clinical and oncological nutrition [3][11].

Moving away from population-based empirical regression equations—which carry high error rates in acute illness and cancer cachexia—focusing on raw bioelectrical parameters (R, X_c, PhA, and ECW/TBW) provides direct information regarding cell membrane capacitance, fluid balance, and tissue viability [1][3][9][11][13][26].

To support the continued translation of bioelectrical impedance from an adjunctive bedside assessment into precision oncology and metabolic medicine, future clinical investigations should focus on four key priorities:

1. Establishing Multi-Ethnic, Population-Specific Normative Percentiles. Multicenter consortia must develop comprehensive reference percentiles for standardized phase angle (SPhA) and BIVA tolerance ellipses, stratified by age, sex, BMI, and ethnicity, establishing universally accepted diagnostic cut-offs for clinical malnutrition and cachexia [1][3][11][19][22][27][32].

doi.org/10.32388/ON9IUN

2. Conducting Interventional Clinical Trials Guided by Bioelectrical Endpoints. Prospective, randomized trials are needed to determine whether bioimpedance-guided nutritional support, targeted antioxidant therapy, and anti-inflammatory interventions can restore membrane capacitance, normalize phase angle trajectories, reduce chemotherapy-induced toxicities, and improve overall survival in oncology cohorts [1][2][13][14][22].
3. Enforcing Hardware Standardization and Metrological Transparency. Device manufacturers should provide open access to raw electrical values (R, X_c, and frequency-dependent impedance data), publish circuit validation procedures using precision test networks, and comply with clinical safety standards (IEC 60601-1), ensuring comparability across commercial platforms [3][11].
4. Implementing Multimodal Morphofunctional Diagnostic Protocols. Clinical nutrition pathways should combine multi-frequency bioelectrical impedance analysis, bedside muscle ultrasound of the rectus femoris, and circulating biomarker panels (CRP, albumin, PNI, cytokine profiles) to form a robust morphofunctional assessment protocol at the point of care [16][23][40].

Statements and Declarations

Funding

The authors received no specific grant, institutional subsidy, or external financial sponsorship from public, commercial, or not-for-profit funding agencies for the design, literature retrieval, writing, or editorial preparation of this manuscript.

Potential Competing Interests

The authors declare that the research was conducted in the absence of any commercial or financial relationships that could be construed as a potential conflict of interest.

Author Contributions

All authors contributed meaningfully to the conceptualization, literature retrieval, thematic synthesis, critical appraisal, and manuscript drafting. All authors reviewed, revised, and approved the final manuscript for publication.

References

1. a, b, c, d, e, f, g, h, i, j, k, l, m, n, o, p, q, r, s, t, u, v, w, x, y, z, ^, ^, ^, ^, ^, ^*da Silva BR, Rufato S, Mialich MS, Cruz LP, Gozzo T, Jordão AA (2023). "Phase Angle Is Related to Oxidative Stress and Antioxidant Biomarkers in Breast Cancer Patients Undergoing Chemotherapy." PLoS One.* ***18****:e0283235. doi:10.1371/journal.pone.0283235.*
2. a, b, c, d, e, f, g, h, i, j*Cvijetić S, Boschiero D, Shin H, Reilly AS, Noorani ST, Vasiljevic N, Ilich JZ (2025). "Extracellular Water and Phase Angle, Markers of Heightened Inflammatory State, and Their Prognostic Potential for Body Composition Outcomes in Adults." Preprints. doi:10.20944/preprints202511.0869.v1.*
3. a, b, c, d, e, f, g, h, i, j, k, l, m, n, o, p, q, r, s, t, u, v, w, x, y, z, ^*Stobäus N, Pirlich M, Valentini L, Schulzke JD, Norman K (2012). "Determinants of Bioelectrical Phase Angle in Disease." Br J Nutr.* ***107****:1217–1220. doi:10.1017/S0007114511004028.*
4. a, b, c, d, e, f, g, h, i, j, k, l, m, n, o, p, q, r, s, t, u, v, w, x, y, z, ^*Barrea L, Muscogiuri G, Pugliese G, Laudisio D, de Alteriis G, Graziadio C, Colao A, Savastano S (2021). "Phase Angle as an Easy Diagnostic Tool of Meta-Inflammation for the Nutritionist." Nutrients.* ***13****(5):1446. doi:10.3390/nu13051446.*
5. a, b, c, d, e, f, g, h*Prete M, Ballarin G, Porciello G, Arianna A, Luongo A, Belli V, Scalfi L, Celentano E (2024). "Bioelectrical Impedance Analysis-Derived Phase Angle (PhA) in Lung Cancer Patients: A Systematic Review." BMC Cancer.* ***24****:608. doi:10.1186/s12885-024-12378-4.*
6. a, b, c, d*de Luis Roman D, López Gómez JJ, Muñoz M, Primo D, Izaola O, Sánchez I (2024). "Evaluation of Muscle Mass and Malnutrition in Patients with Colorectal Cancer Using the Global Leadership Initiative on Malnutrition Criteria and Comparing Bioelectrical Impedance Analysis and Computed Tomography Measurements." Nutrients.* ***16****(17):3035. doi:10.3390/nu16173035.*
7. a, b*Vieira Maroun E, Argente Pla M, Pedraza Serrano MJ, Muresan BT, Ramos Prol A, Gascó Santana E, Martín Sanchis S, Durá De Miguel Á, Micó García A, Cebrián Vázquez A, Durbá Lacruz A, Merino-Torres JF (2025). "Phase Angle and Ultrasound Assessment of the Rectus Femoris for Predicting Malnutrition and Sarcopenia in Patients with Esophagogastric Cancer: A Cross-Sectional Pilot Study." Nutrients.* ***17****(1):91. doi:10.3390/nu17010091.*
8. a, b*Gupta D, Lammersfeld CA, Burrows JL, Dahlk SL, Vashi PG, Grutsch JF, Hoffman S, Lis CG (2004). "Bioelectrical Impedance Phase Angle in Clinical Practice: Implications for Prognosis in Advanced Colorectal Cancer2." Am J Clin Nutr.* ***80****:1634–1638. doi:10.1093/ajcn/80.6.1634.*
9. a, b, c, d, e, f, g, h, i, j, k, l, m, n, o, p, q, r, s, t, u, v, w, x, y, z, ^, ^, ^, ^, ^, ^, ^, ^, ^, ^, ^, ^, ^, ^, ^, ^, ^, ^, ^*Barrea L, Muscogiuri G, Laudisio D, Di Somma C, Salzano C, Pugliese G, de Alteriis G, Colao A, Savastano S (2019). "Phase Angle: A Possible Biomarker to Quantify Inflammation in Subjects with Obesity and 25(OH) D Deficiency." Nutrie*

*nts. **11**. doi:10.3390/nu11081747.*

10. [a, b, c, d, e] *Barazzoni R, Jensen GL, Correia MITD, Gonzalez MC, Higashiguchi T, Shi HP, Bischoff SC, Boirie Y, Carrasco F, Cruz-Jentoft A, Fuchs-Tarlovsky V, Fukushima R, Heymsfield S, Mourtzakis M, Muscaritoli M, Norman K, Nyulasi I, Pisprasert V, Prado C, De van der Schueren M, Yoshida S, Yu J, Cederholm T, Compher C (2022). "Guidance for Assessment of the Muscle Mass Phenotypic Criterion for the Global Leadership Initiative on Malnutrition (GLIM) Diagnosis of Malnutrition." Clin Nutr. **41**:1425–1433. doi:10.1016/j.clnu.2022.02.001.*
11. [a, b, c, d, e, f, g, h, i, j, k, l, m, n, o, p, q, r, s, t, u, v, w, x, y, z, ^] *da Silva BR, Orsso CE, Gonzalez MC, Sicchieri JMF, Mialich MS, Jordao AA, Prado CM (2023). "Phase Angle and Cellular Health: Inflammation and Oxidative Damage." Rev Endocr Metab Disord. **24**:543–562. doi:10.1007/s11154-022-09775-0.*
12. [a, b, c, d] *Lee GR, Kim EY (2023). "Usefulness of Phase Angle on Bioelectrical Impedance Analysis as a Surveillance Tool for Postoperative Infection in Critically Ill Patients." Front Med (Lausanne). **10**:1111727. doi:10.3389/fmed.2023.1111727.*
13. [a, b, c, d, e, f] *Kyle UG, Bosaeus I, De Lorenzo AD, Deurenberg P, Elia M, Manuel Gómez J, Lilienthal Heitmann B, Kent-Smith L, Melchior JC, Pirlich M, Scharfetter H, AMWJS, Pichard C (2004). "Bioelectrical Impedance Analysis-Part II: Utilization in Clinical Practice." Clin Nutr. **23**:1430–1453. doi:10.1016/j.clnu.2004.09.012.*
14. [a, b, c] *Kyle UG, Bosaeus I, De Lorenzo AD, Deurenberg P, Elia M, Gómez JM, Heitmann BL, Kent-Smith L, Melchior JC, Pirlich M, Scharfetter H, Schols AM, Pichard C (2004). "Bioelectrical Impedance Analysis--Part I: Review of Principles and Methods." Clin Nutr. **23**:1226–1243. doi:10.1016/j.clnu.2004.06.004.*
15. [a, b, c, d, e] *Marra M, Sammarco R, De Lorenzo A, Iellamo F, Siervo M, Pietrobelli A, Donini LM, Santarpia L, Cataldi M, Pasanisi F, Contaldo F (2019). "Assessment of Body Composition in Health and Disease Using Bioelectrical Impedance Analysis (BIA) and Dual Energy X-Ray Absorptiometry (DXA): A Critical Overview." Contrast Media Mol Imaging. **2019**:3548284. doi:10.1155/2019/3548284.*
16. [a, b, c, d, e, f, g, h, i, j, k] *Diniz MEO, Almeida LFM, Araújo VGS, Teixeira FG, Coelho CDF, Lopes-Martins RAB (2025). "Bioelectrical Impedance Analysis and Phase Angle in Cancer Care: Prognosis, Nutrition, and Clinical Utility in 19.151 Patient." Preprints. doi:10.20944/preprints202511.1288.v1.*
17. [^] *Baethge CG-W, Sandra, Mertens, Stephen (2019). "SANRA-a Scale for the Quality Assessment of Narrative Review Articles." Res Integr Peer Rev. **4**:5. doi:10.1186/s41073-019-0064-8.*
18. [^] *Jirků J, Křížová J (2025). "Phase Angle in Bioelectrical Impedance: New Perspectives in Health and Body Composition Assessment." Physiol Res. **74**:1007–1019. doi:10.33549/physiolres.935629.*
19. [a, b, c, d, e, f, g] *Nwosu AC, Mayland CR, Mason S, Cox TF, Varro A, Stanley S, Ellershaw J (2019). "Bioelectrical Impedance Vector Analysis (BIVA) as a Method to Compare Body Composition Differences According to Cancer Stage and Type." Clin Nutr ESPEN. **30**:59–66. doi:10.1016/j.clnesp.2019.02.006.*
20. [a, b, c, d, e, f, g, h, i, j] *Tsigos C, Stefanaki C, Lambrou G, Boschiero D, Chrousos G (2015). "Stress and Inflammatory Biomarkers and Symptoms Are Associated with Bioimpedance Measures." Eur J Clin Invest. **45**:126–134. doi:10.1111/eci.12388.*
21. [a, b, c, d] *Abasi S, Aggas JR, Garayar-Leyva GG, Walther BK, Guiseppi-Elie A (2022). "Bioelectrical Impedance Spectroscopy for Monitoring Mammalian Cells and Tissues under Different Frequency Domains: A Review." ACS Measurement Science Au. **2**:495–516. doi:10.1021/acsmeasuresciau.2c00033.*
22. [a, b, c, d, e, f] *Cereda E, Casirati A, Klersy C, Nardi M, Vandoni G, Agnello E, Crotti S, Masi S, Ferrari A, Pedrazzoli P, Caccialanza R, Caccialanza R, Cereda E, Casirati A, Crotti S, Masi S, Klersy C, Ferrari A, Pedrazzoli P, Gavazzi C, Vandoni G, Farina G, La Verde N, Zagonel V, Nardi MT, Baldan I, Di Costanzo F, Mascheroni A, Trestini I, Valoriani F, Lucchin L, Aprile G, De Francesco A, Agnello E, Giovanardi F (2024). "Bioimpedance-Derived Body Composition Parameters Predict Mortality and Dose-Limiting Toxicity: The Multicenter ONCO-BIVA Study." ESMO Open. **9**:103666. doi:10.1016/j.esmoop.2024.103666.*
23. [a, b, c, d, e, f, g, h, i, j, k] *Dalla Rovere L, Tapia Guerrero MJ, Doulatram-Gamgaram VK, Garcia-Olivares M, del Arco-Romualdo B, Gonzalo-Marín M, Mora MR, Decoud DB, Aizpún CD, Sánchez-Torralvo FJ, Herola-Cobos C, Hardy-Añón C, Hernandez-Sanchez A, García-Almeida JM, Olveira G (2026). "Bioelectrical Impedance and GLIM Criteria Identify Early Nutritional Deterioration and Mortality in Acute Leukemia Patients Undergoing Chemotherapy." Nutrients. **18(3)**:374. doi:10.3390/nu18030374.*
24. [^] *Cotogni P, Monge T, Fadda M, De Francesco A (2018). "Bioelectrical Impedance Analysis for Monitoring Cancer Patients Receiving Chemotherapy and Home Parenteral Nutrition." BMC Cancer. **18**:990. doi:10.1186/s12885-018-4904-6.*
25. [a, b, c] *Branco MG, Mateus C, Capelas ML, Pimenta N, Santos T, Mäkitie A, Ganhão-Arranhado S, Trabulo C, Ravasco P (2023). "Bioelectrical Impedance Analysis (BIA) for the Assessment of Body Composition in Oncology: A Scoping Review." Nutrients. **15**. doi:10.3390/nu15224792.*
26. [a, b, c, d] *Dupertuis YM, Jimaja W, Beardsley Levoy C, Genton L (2025). "Bioelectrical Impedance Analysis Instruments: How Do They Differ, What Do We Need for Clinical Assessment?" Curr Opin Clin Nutr Metab Care. **28**:379–387. doi:10.1097/mco.0000000000001142.*
27. [a, b, c, d, e, f] *Dal Bello S, Ceccarelli L, Tereshko Y, Gigli GL, D'Anna L, Valente M, Merlino G (2025). "Prognostic Impact of Malnutrition Evaluated via Bioelectrical Impedance Vector Analysis (BIVA) in Acute Ischemic Stroke: Findings from an Inverse Probability Weighting Analysis." Nutrients. **17(5)**:919. doi:10.3390/nu17050919.*

28. ^Piccoli A, Rossi B, Pillon L, Bucciante G (1994). "A New Method for Monitoring Body Fluid Variation by Bioimpedance Analysis: The RXc Graph." Kidney Int. **46**:534–539. doi:10.1038/ki.1994.305.

29. ^Piccoli AN, S, Caberlotto A, Bottazzo S, Rossi B, Pillon L, Maggiore Q. "Bivariate Normal Values of the Bioelectrical Impedance Vector in Adult and Elderly Populations." Am J Clin Nutr. **61**:269–270. doi:10.1093/ajcn/61.2.269.

30. ^Campa F, Coratella G, Cerullo G, Stagi S, Paoli S, Marini S, Grigoletto A, Moroni A, Petri C, Andreoli A, Ceolin C, Degan R, Izzicupo P, Sergi G, Mascherini G, Micheletti Cremasco M, Marini E, Toselli S, Moro T, Paoli A (2023). "New Bioelectrical Impedance Vector References and Phase Angle Centile Curves in 4,367 Adults: The Need for an Urgent Update after 30 Years." Clin Nutr. **42**:1749–1758. doi:10.1016/j.clnu.2023.07.025.

31. ^Piccoli A, Pillon L, Dumler F (2002). "Impedance Vector Distribution by Sex, Race, Body Mass Index, and Age in the United States: Standard Reference Intervals as Bivariate Z Scores." Nutrition. **18**:153–167. doi:10.1016/S0899-9007(01)00665-7.

32. a, b, cCeolin J, de Borba EL, Mundstock E, de Oliveira JR, Mattiello R, Bodanese LC (2023). "Phase Angle of Bioimpedance as a Marker of Inflammation in Cardiovascular Diseases: A Systematic Review." Nutrition. **112**:112064. doi:10.1016/j.nut.2023.112064.

33. a, bSwaraj S, Marx G, Masterson G, Leuwer M (2003). "Bioelectrical Impedance Analysis as a Predictor for Survival in Patients with Systemic Inflammatory Response Syndrome." Critical Care. **7**:P185. doi:10.1186/cc2074.

34. a, bAyala A, Muñoz MF, Argüelles S (2014). "Lipid Peroxidation: Production, Metabolism, and Signaling Mechanisms of Malondialdehyde and 4-Hydroxy-2-Nonenal." Oxid Med Cell Longev. **2014**:360438. doi:10.1155/2014/360438.

35. ^Ballmer PE (2001). "Causes and Mechanisms of Hypoalbuminaemia." Clin Nutr. **20**:271–273. doi:10.1054/clnu.2001.0439.

36. ^Fleck A, Hawker F, Wallace PI, Raines G, Trotter J, Ledingham IM, Calman KC (1985). "INCREASED VASCULAR PERMEABILITY: A MAJOR CAUSE OF HYPOALBUMINAEMIA IN DISEASE AND INJURY." The Lancet. **325**:781–784. doi:10.1016/S0140-6736(85)91447-3.

37. ^Santarpia L, Marra M, Montagnese C, Alfonsi L, Pasanisi F, Contaldo F (2009). "Prognostic Significance of Bioelectrical Impedance Phase Angle in Advanced Cancer: Preliminary Observations." Nutrition. **25**:930–931. doi:10.1016/j.nut.2009.01.015.

38. a, bOnodera T, GN, Kosaki G (1984). "Prognostic Nutritional Index in Gastrointestinal Surgery of Malnourished Cancer Patients." Nihon Geka Gakkai Zasshi [Journal of Japan Surgical Society]. 1001–1005.

39. ^Nozoe T, Ninomiya M, Maeda T, Matsukuma A, Nakashima H, Ezaki T (2010). "Prognostic Nutritional Index: A Tool to Predict the Biological Aggressiveness of Gastric Carcinoma." Surg Today. **40**:440–443. doi:10.1007/s00595-009-4065-y.

40. a, b, c, d, eTomasiewicz A, Targowski T, Makuch S, Polański J, Tański W (2025). "The Relationship Between Bioelectrical Impedance Analysis Parameters and Laboratory Biomarkers in an Elderly Polish Cohort: A Cross-Sectional Study." Nutrients. **17**. doi:10.3390/nu17243843.

41. ^Bobos M, Stevanovic P, Zivic R, Dimic N, Djuric M, Nenadic I, Mijovic M, Vasic A, Lalosevic M, Borocki K, Stevanovic V, Mutavdzin Krneta S (2025). "Concurrent Validity of GLIM Criteria in Nutritional Assessment of Surgical Patients with Colorectal Cancer." Front Nutr. **12**:1691041. doi:10.3389/fnut.2025.1691041.

42. ^López-Gómez JJ, García-Beneitez D, Jiménez-Sahagún R, Izaola-Jauregui O, Primo-Martín D, Ramos-Bachiller B, Gómez-Hoyos E, Delgado-García E, Pérez-López P, De Luis-Román DA (2023). "Nutritional Ultrasonography, a Method to Evaluate Muscle Mass and Quality in Morphofunctional Assessment of Disease Related Malnutrition." Nutrients. **15**(18):3923. doi:10.3390/nu15183923.

43. ^García-Almeida JM, García-García C, Vegas-Aguilar IM, Ballesteros Pomar MD, Cornejo-Pareja IM, Fernández Medina B, de Luis Román DA, Bellido Guerrero D, Bretón Lesmes I, Tinahones Madueño FJ (2023). "Nutritional Ultrasound®: Conceptualisation, Technical Considerations and Standardisation." Endocrinología, Diabetes y Nutrición [Endocrinology, Diabetes and Nutrition]. **70**:74–84. doi:10.1016/j.endinu.2022.03.008.

Declarations

Funding: No specific funding was received for this work.

Potential competing interests: No potential competing interests to declare.